A Multistage Distributionally Robust Optimization Approach for Generation Dispatch with Demand Response under Endogenous and Exogenous Uncertainties

Yiwen Huang[1], Wentao Huang[1], Nengling Tai[1], Canbing Li[1], Ran Li[1], and Moduo Yu[1]

[1]Shanghai Jiao Tong University

July 10, 2023

Abstract

Decision-dependent (endogenous) uncertainties (DDUs), as a new type of uncertainties revealed recently, couple dispatch decisions with uncertainty parameters and thus render power system dispatch more challenging. However, most previous works handled various DDUs via stochastic programming (SP) or robust optimization (RO) in a two-stage framework, which undoubtedly introduces the drawbacks of SP and RO, and cannot meet the nonanticipativity requirements in power scheduling. In this paper, we propose a multistage distributionally robust optimization (DRO) method for generation dispatch with demand response (DR) considering the DDUs of deferrable loads and the decision-independent (exogenous) uncertainties (DIUs) of wind power and regular loads. By analyzing the structure of decision-dependency parameters, a novel data-driven decision-dependent ambiguity set is proposed, which provides a generic framework for formulating DDUs and DIUs simultaneously. Then a multistage DRO model with nested max-min structure is developed to integrate the merits of DRO and nonanticipativity into generation dispatch. The proposed model is solved by tailored reformulation method and improved stochastic dual dynamic integer programming (SDDiP). Case studies illustrate the effectiveness of the proposed approach by comparing with the multistage SP, RO, and decision-independent DRO methods.

ISSN 1751-8644
doi: 0000000000
www.ietdl.org

A Multistage Distributionally Robust Optimization Approach for Generation Dispatch with Demand Response under Endogenous and Exogenous Uncertainties

Yiwen Huang[1], *Wentao Huang*[1*], *Nengling Tai*[1,2], *Canbing Li*[1], *Ran Li*[1], *Moduo Yu*[1]

[1] *Department of Electrical Engineering, Shanghai Jiao Tong University, Shanghai, China*
[2] *College of Smart Energy, Shanghai Jiao Tong University, Shanghai, China*
* *E-mail: hwt8989@sjtu.edu.cn*

Abstract: Decision-dependent (endogenous) uncertainties (DDUs), as a new type of uncertainties revealed recently, couple dispatch decisions with uncertainty parameters and thus render power system dispatch more challenging. However, most previous works handled various DDUs via stochastic programming (SP) or robust optimization (RO) in a two-stage framework, which undoubtedly introduces the drawbacks of SP and RO, and cannot meet the nonanticipativity requirements in power scheduling. In this paper, we propose a multistage distributionally robust optimization (DRO) method for generation dispatch with demand response (DR) considering the DDUs of deferrable loads and the decision-independent (exogenous) uncertainties (DIUs) of wind power and regular loads. By analyzing the structure of decision-dependency parameters, a novel data-driven decision-dependent ambiguity set is proposed, which provides a generic framework for formulating DDUs and DIUs simultaneously. Then a multi-stage DRO model with nested max-min structure is developed to integrate the merits of DRO and nonanticipativity into generation dispatch. The proposed model is solved by tailored reformulation method and improved stochastic dual dynamic integer programming (SDDiP). Case studies illustrate the effectiveness of the proposed approach by comparing with the multistage SP, RO, and decision-independent DRO methods.

Nomenclature

Abbreviations

SP	Stochastic programming
RO	Robust optimization
DRO	Distributionally robust optimization
PDF	Probability distribution function
DDU	Decision-dependent uncertainty
DIU	Decision-independent uncertainty
DR	Demand response
SDDP	Stochastic dual dynamic programming
SDDiP	Stochastic dual dynamic integer programming
MILP	Mixed integer linear programming

Indices and Sets

t, τ, $\mathcal{T}$	Index/set of time periods
i, $\mathcal{G}$	Index/set of thermal units
h, $\mathcal{W}$	Index/set of wind farms
m, $\mathcal{D}_s$	Index/set of deferrable loads
n, $\mathcal{D}_r$	Index/set of regular loads
l, $\mathcal{L}$	Index/set of transmission lines
k	Index of segments in binary expansion
$d, j, v, \mathcal{U}$	Index/set of random variables, $\mathcal{U} = \mathcal{D}_s \cup \mathcal{D}_r \cup \mathcal{W}$

Parameters

α_i	Generation cost coefficient of thermal unit i
$\beta_i^{\pm}$	Upward/downward reserve cost coefficient of thermal unit i
$d_i^{\pm}$	Upward/downward regulation cost coefficient of thermal unit i
P_i^u, P_i^l	Maximum/minimum output of thermal unit i
$\mathcal{R}_i^u, \mathcal{R}_i^d$	Upward/downward ramping limits of thermal unit i
c^{ls}	Penalty cost coefficient for load shedding
c_m^s	Cost coefficient for demand shifting of deferrable load m
c_n^c	Cost coefficient for demand curtailment of regular load n
F_l	Power flow capacity of transmission l
$w_{h,t}^f$	Forecast output of wind farm h at time t
$D_{m,t}^{s,f}$	Forecast demand of deferrable load m at time t
$D_{n,t}^{r,f}$	Forecast demand of regular load n at time t
$\pi_{(\cdot)l}$	Power transfer distribution factors
$d_{m,t,\tau}^{s,u}$	Upper bound on the demand shifting of deferrable load m from time t to τ
$d_{n,t}^{c,u}$	Upper bound on the demand curtailment of regular load n at time t
λ_d^{μ},$\boldsymbol{\lambda}_d^{cov}$	Decision-dependency coefficients

Decision Variables

$p_{i,t}$	Pre-dispatched power of thermal unit i at time t
$r_{i,t}^{\pm}$	Reserve capacity of thermal unit i at time t
$\hat{w}_{h,t}$	Dispatched wind power of wind farm h at time t in pre-dispatch stage
$p_{i,t}^{\pm}$	Upward/downward regulation power of thermal unit i at time t
$w_{h,t}$	Dispatched wind power of wind farm h at time t in re-dispatch stage
$d_{m,t,\tau}^s$	Demand shifting of deferrable load m from time t to τ
$d_{n,t}^c$	Demand curtailment of regular load n at time t
$d_{m,t}^{s,ls}$,$d_{n,t}^{r,ls}$	Load shedding of deferrable load m and regular load n at time t
γ,$\boldsymbol{\varphi}$,$\boldsymbol{\psi}$	Dual variables corresponding to the constraints in ambiguity sets
$\boldsymbol{z}_{t-1}^{(\cdot),copy}$	Dummy variables

Random Variables

$w_{h,t}^o$	Actual output of wind farm h at time t
$D_{m,t}^s$	Actual demand of deferrable load m at time t
$D_{n,t}^r$	Actual demand of regular load n at time t

1 Introduction

The modern power systems are undergoing the transformation towards high renewable penetration. Nevertheless, the inherent variability and unpredictability of renewable energy and loads pose great challenges to power systems scheduling. How to hedge against uncertainties and increase the robustness and economic performance of dispatch solutions have become widely studied problems for decades.

In the existing works, three commonly used approaches to tackle uncertainties are stochastic programming (SP) [1], [2], robust optimization (RO) [3], [4], and distributionally robust optimization (DRO) [5], [6]. Stochastic programming aims to minimize the expected costs given representative scenarios with known probability distribution functions (PDF), but the perfect information of PDF is hard to obtain in practical scheduling. Robust optimization finds the optimal solution under the worst-case scenario in the uncertainty set. Since the worst-case scenario always occurs at the bound of uncertainty set with low occurrence probability, the solutions of RO may be over-conservative. To bridge the gap between SP and RO, DRO assumes that ambiguously known PDF lies within a family of candidate distributions, namely the ambiguity set, and the optimal solution is sought for the worst-case probability distribution within the ambiguity set. Since the DRO method neither requires the full knowledge of PDF nor pessimistically seeks solutions under the worst-case scenario, a satisfactory trade-off between robustness and economics is obtained.

Although SP, RO and DRO have been applied to power system scheduling, most of existing works adopted two-stage frameworks. Specifically, the day-ahead scheduling determines unit commitment, generation strategy or economic dispatch based on the forecast renewable output and loads. And the intra-day re-dispatch utilizes flexible resources to hedge against any uncertainties, where the uncertainty realizations at all time periods are assumed to be observed simultaneously. However, in practice, the uncertainty at each time period is observed sequentially and the dispatch decisions are made period-by-period based on the revealed uncertainties. Such time logic and causality are called nonanticipativity [7]. In this regard, the two-stage method does not respect the fact of sequential decision-making in power scheduling.

To solve this issue, multistage scheduling is proposed recently, where the current decision relies only on the uncertainties up to now instead of future information. Thus, the multistage approach can effectively meet the nonanticipativity requirements in power scheduling. Reference [8] proposed a multistage stochastic energy and reserve dispatch model based on stochastic dual dynamic programming (SDDP). In [9], a multistage SP with stochastic dual dynamic integer programming (SDDiP) was proposed for multi-period active distribution network planning. For RO-based method, reference [10] proposed a multistage robust network-constrained unit commitment model with non-fixed recourse. In [11], a multistage robust scheduling model is proposed for regional power grids considering uncertain sequential outages and renewable-load power. A multistage robust resilient scheduling model with binary recourses is developed in [12] for regional power grids considering sequential realizations of uncertainties under tropical cyclone. Besides, reference [13] developed a multistage DRO model for multiperiod economic dispatch with virtual energy storage.

In the above literature, the involved uncertainties are exogenous, i.e., the uncertainty parameters are predetermined and fixed before the decision process. However, recent studies have revealed another important type of uncertainty in power systems, referring to endogenous uncertainty, also called decision-dependent uncertainty (DDU). DDUs indicate that the dispatch decisions will affect the property of uncertainties, including the timing when the uncertainties are resolved (type-1) [14], or the distribution characteristics of random variables (type-2) [15]. DDUs have got increasing attention in power systems in recent years. Reference [15] proposed a stochastic wind farm expansion planning model where the decision-dependency between wind power output prediction errors and wind farm size caused by spatial smoothing effect is considered. In [16], the impact of enhancement measures on the failure probability of transmission lines is formulated, and a two-stage SP model was developed for transmission defense hardening problem. Reference [17] formulated the dependency between operation decisions and device reliability parameters, with which a two-stage stochastic unit commitment model is established to quantify the power system operational reliability. In [18], a robust scheduling model of virtual power plant is proposed under the DDUs of real-time reserve deployment requests and the decision-independent uncertainties (DIUs) of market clearing prices and wind power. In [19], strategic day-ahead renewable power curtailment is considered in robust generation dispatch, which affects the variation range of real-time wind power output and thus forms a decision-dependent uncertainty set. Reference [20] developed a multistage robust dispatch model to cope with the DDUs of deferrable loads.

The aforementioned works have significantly contributed to the research on the DDUs in power systems. However, all of them almost adopted SP or RO methods in a two-stage framework. Reference [20] used a multistage dispatch method but it still belongs to the category of RO. In this case, the mentioned drawbacks of SP, RO and two-stage scheduling might be inherently introduced into dispatch decisions. To fully integrate robustness, economics and nonanticipativity into power systems, it is necessary to develop a DRO-based multistage scheduling method for handling both DDUs and DIUs. However, the research that addresses DDUs and DIUs in power systems via a multistage DRO approach is limited. In [21], a multistage distributionally robust model with three types decision-dependent ambiguity sets was proposed. Nevertheless, only DDUs are considered in the ambiguity sets, which cannot be directly applied to the case where both DDUs and DIUs need to be modeled by the covariance matrix in ambiguity sets.

To fill the research gap, this paper proposes a multistage distributionally robust generation dispatch model with demand response (DR) considering the DDUs of deferrable loads and the DIUs of wind power and regular loads. The contributions of this paper are summarized as follows:

(1) By analyzing the structural characteristic of decision-dependency parameters when DDUs and DIUs are combined, a novel decision-dependent ambiguity set is proposed to formulate the DDUs of deferrable loads and the DIUs of wind power and regular loads simultaneously. Moreover, a data-driven approach is offered based on real-world data to obtain decision-dependency parameters in practical engineering.

(2) A multistage distributionally robust generation dispatch model with DR is proposed considering both DDUs and DIUs, which fully leverages the merits of DRO to enhance the robustness and economic of dispatch solutions under DDUs and DIUs, while ensuring nonanticipativity through the multistage scheduling process.

(3) The proposed multistage DRO model is computationally intractable due to nested optimization structure and decision-dependent ambiguity set. To this end, a tailored reformulation method is developed to derive the original model into a tractable mixed integer linear programming (MILP). Then an improved SDDiP algorithm with introduced dummy variables to effectively solve the model.

The rest of this paper is organized as follows. Section 2 formulates the decision-dependent ambiguity set and the multistage distributionally robust generation dispatch model. Section 3 provides the reformulation of the multistage DRO model and the improved SDDiP algorithm. Section 4 presents the numerical experiments. Section 5 concludes this paper.

2 Mathematical Formulation

2.1 Problem Description and Scheduling Framework

In this paper, we consider a multistage generation dispatch problem for a power system with thermal generators, wind farms and loads participating in DR programs. The pre-dispatch in day-ahead determines the power output and reserve capacity of thermal units

IET Research Journals, pp. 1–11

according to forecast wind power and loads. The re-dispatch in intra-day is formulated as a sequential decision-making process with T stages. At each stage, the optimal decision including up- and down-regulation power of thermal units, dispatched wind power, demand shifting of deferrable loads, demand curtailment of curtailable loads and load shedding are determined based on observed uncertainties.

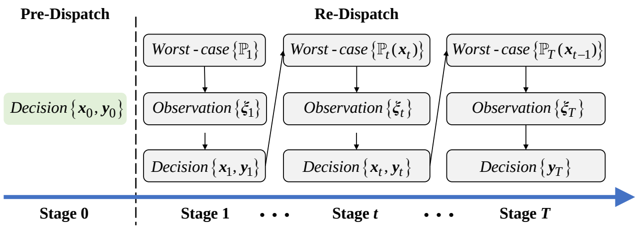

Fig. 1: Sequential decision-making process of the multistage DRO model with decision-dependent ambiguity set.

The stated multistage decision-making process is shown in Fig. 1. With the pre-dispatch decisions obtained in day-ahead, the re-dispatch decisions are determined dynamically at each stage. Specifically, we make the decision $\{\boldsymbol{x}_1, \boldsymbol{y}_1\}$ when the uncertainty $\boldsymbol{\xi}_1$ is observed at stage 1. The dispatch decision $\boldsymbol{x}_1$ affects the worst-case probability distribution $\boldsymbol{\xi}_2$ due to the decision-dependent ambiguity set, under which the uncertainty $\boldsymbol{\xi}_2$ is observed and then the corresponding decision $\{\boldsymbol{x}_2, \boldsymbol{y}_2\}$ are made at stage 2. Such a dynamic process continues until reaching stage T.

2.2 Modeling DDU and DIU via Data-Driven Decision-Dependent Ambiguity Set

2.2.1 Constructing Decision-Dependent Ambiguity Set

In this subsection, the DDUs of deferrable loads and the DIUs of wind power and regular loads are formulated via the data-driven decision-dependent ambiguity set. Note that the regular loads in this paper include the curtailable loads participating in DR and the conventional loads not participating in DR. Since the two types of loads are both belong to DIUs, they are uniformly called regular loads for the sake of notion simplicity. The conventional loads can be distinguished with the curtailable loads by setting the parameter $d_{n,t}^{c,u}$ in equation (6e) to be 0.

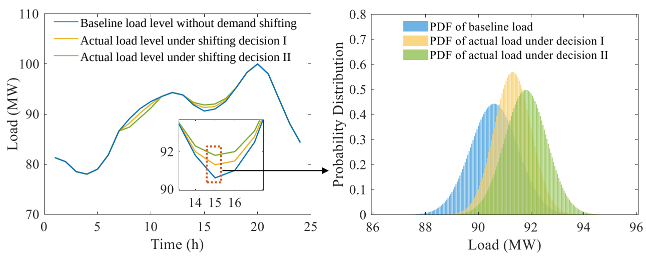

Fig. 2: Illustration of decision-dependent distribution parameters of deferrable load uncertainties.

The DDUs of deferrable loads are essentially caused by the accumulation of demand shifting decisions at previous stages [20]. For a real-time DR program in re-dispatch, the demands at current time will be shifted to the future time. We denote the original baseline level of deferrable load m at time t without demand shifting as $\hat{D}_{m,t}^s$. With the transferred demands at previous time periods, the actual load level at current time t is stated as

$$D_{m,t}^s = \hat{D}_{m,t}^s + \sum_{\tau=1}^{t-1} d_{m,\tau,t}^s, \forall m \in \mathcal{D}_s \tag{1}$$

Based on equation (1), the uncertain deferrable loads will fluctuate up and down around the actual load level $D_{m,t}^s$. Thus, the uncertainty parameters of deferrable loads are affected by the demand shifting decisions at the previous stages. Fig. 2 intuitively illustrates the decision-dependent distribution information of deferrable loads under different demand shifting decisions.

In addition to the DDUs of deferrable loads, another important uncertainties in power systems are wind power and regular loads, which belong to DIUs. To enhance the robustness of power systems under DDUs and DIUs, it is necessary to develop an ambiguity set that contains both types of uncertainties. To this end, a moment-based decision-dependent ambiguity set is proposed in this section, which can formulate the DDUs of deferrable loads and the DIUs of wind power and regular loads simultaneously. The decision-dependent ambiguity set is written as follows

$$\mathcal{P}_t\left(\boldsymbol{d}_{[t-1],t}^s\right) = \left\{\mathbb{P}\ \middle|\ \begin{array}{l} \Pr\left(\boldsymbol{\xi}_t \in \Omega_t\right) = 1 \\ \mathbb{E}_{\mathbb{P}}\left(\boldsymbol{\xi}_t\right) = \boldsymbol{\mu}\left(\boldsymbol{d}_{[t-1],t}^s\right) \\ \mathbb{E}_{\mathbb{P}}\left[\left(\boldsymbol{\xi}_t - \boldsymbol{\mu}\left(\boldsymbol{d}_{[t-1],t}^s\right)\right)\left(\boldsymbol{\xi}_t - \boldsymbol{\mu}\left(\boldsymbol{d}_{[t-1],t}^s\right)\right)^T\right] \\ \qquad = \Sigma\left(\boldsymbol{d}_{[t-1],t}^s\right) \end{array}\right. \tag{2}$$

where $\boldsymbol{\xi}_t = \left\{D_{m,t}^s, w_{h,t}^o, D_{n,t}^r\right\}$ represents random variables including deferrable loads $D_{m,t}^s$, wind power $w_{h,t}^o$ and regular loads $D_{n,t}^r$. $\boldsymbol{d}_{[t-1],t}^s = \left\{\boldsymbol{d}_{1,t}^s, \boldsymbol{d}_{2,t}^s, ..., \boldsymbol{d}_{t-1,t}^s\right\}$ denotes transferred demands from previous time $1, \ldots, t-1$ to current time t, where $\boldsymbol{d}_{\tau,t}^s = \left\{d_{1,\tau,t}^s, ..., d_{m,\tau,t}^s\right\}$.

The second and third lines of (2) couples the demand shifting decisions $d_{d,\tau,t}^s$ with the mean vector $\boldsymbol{\mu}\left(\boldsymbol{d}_{[t-1],t}^s\right)$ and covariance matrix $\Sigma\left(\boldsymbol{d}_{[t-1],t}^s\right)$, which are formulated as follows

$$\begin{cases} \mu_d\left(\boldsymbol{d}_{[t-1],t}^s\right) = \hat{\mu}_d\left(1 + \sum_{\tau=1}^{t-1} \lambda_d^\mu d_{d,\tau,t}^s\right), \forall d \in \mathcal{D}_s \\ \mu_j\left(\boldsymbol{d}_{[t-1],t}^s\right) = \hat{\mu}_j, \forall j \in \mathcal{D}_r \cup \mathcal{W} \end{cases} \tag{3a}$$

$$\Sigma\left(\boldsymbol{d}_{[t-1],t}^s\right) = \hat{\Sigma} + \sum_{d \in \mathcal{D}_s} \sum_{\tau=1}^{t-1} \boldsymbol{\lambda}_d^{cov} d_{d,\tau,t}^s \tag{3b}$$

where $\hat{\mu}_d$ and $\hat{\Sigma}$ are the mean and covariance matrix calculated by using the data of wind power, regular load and baseline deferrable loads. The baseline loads refer to the deferrable loads without any demand shifting, which can be estimated by the methods in exiting literature [22], [23]. λ_d^μ is decision-dependency coefficient that measures the impact of demand shifting decision of deferrable load d on its mean μ_d, reflecting DDU. λ_j^μ is 0 when j represents wind farms or regular loads, reflecting DIU. $\boldsymbol{\lambda}_d^{cov}$ is the decision-dependency coefficient matrix. Since both DDUs and DIUs are considered in $\Sigma\left(\boldsymbol{d}_{[t-1],t}^s\right)$ but only the part that is related to DDUs will be affected by demand shifting decisions, an analysis on the structure of $\boldsymbol{\lambda}_d^{cov}$ should be conducted. We use the following example to illustrate that.

Example 1. *Suppose there are two deferrable loads, one wind farm and one regular load. The random variable vector is stated as* $\boldsymbol{\xi} = \left(D_1^s, D_2^s, w_1^o, D_1^r\right)^{\mathrm{T}}$ *. Based on the calculation way of covariance matrix* $\Sigma\left(\boldsymbol{d}_{[t-1],t}^s\right)$ *shown in (2), we can see that the demand shifting decision* $d_{d,\tau,t}^s$ *only affects the rows and columns related to deferrable load in covariance matrix* $\Sigma\left(\boldsymbol{d}_{[t-1],t}^s\right)$*. In this example, since the random variables of deferrable load* $\left(D_1^s, D_2^s\right)$ *are the first two elements of* $\boldsymbol{\xi}$*, only the first and second row/column* *of* $\Sigma\left(\boldsymbol{d}^s_{[t-1],t}\right)$ *will be affected by demand shifting decisions. Thus, the coefficient matrix* $\boldsymbol{\lambda}^{cov}_d$ *in (3b) has the following structure in this example*

$$\begin{aligned}
\boldsymbol{\lambda}^{cov}_1 &= \begin{pmatrix} \lambda^{cov}_{1,11} & \lambda^{cov}_{1,12} & \lambda^{cov}_{1,13} & \lambda^{cov}_{1,14} \\ \lambda^{cov}_{1,21} & 0 & 0 & 0 \\ \lambda^{cov}_{1,31} & 0 & 0 & 0 \\ \lambda^{cov}_{1,41} & 0 & 0 & 0 \end{pmatrix} \\
\boldsymbol{\lambda}^{cov}_2 &= \begin{pmatrix} 0 & \lambda^{cov}_{2,12} & 0 & 0 \\ \lambda^{cov}_{2,21} & \lambda^{cov}_{2,22} & \lambda^{cov}_{2,23} & \lambda^{cov}_{2,24} \\ 0 & \lambda^{cov}_{2,32} & 0 & 0 \\ 0 & \lambda^{cov}_{2,42} & 0 & 0 \end{pmatrix}
\end{aligned} \tag{3c}$$

In Example 1, only the d^{th} row and d^{th} column of $\boldsymbol{\lambda}^{cov}_d$ are non-zero. This structural characteristic of $\boldsymbol{\lambda}^{cov}_d$ is consistent with the fact that the demand shifting decisions will only affect the uncertainties of deferrable loads, while the uncertainties of wind power and regular loads are independent to the demand shifting decisions. Thus, such special structure of $\boldsymbol{\lambda}^{cov}_d$ can provide a generic framework to formulate DDUs and DIUs simultaneously in the ambiguity set while allowing us to distinguish them.

From this perspective, we can see the difference between our ambiguity set and the decision-dependent ambiguity set in [21]. Specifically, the ambiguity set in [21] only considers the DDUs and each elements of covariance matrix will be affected by decisions. Thus, the decision-dependency coefficient λ^{cov}_d in [21] is a constant. However, the situation becomes different in our study when DDUs and DIUs are combined. Since only part of $\Sigma\left(\boldsymbol{d}^s_{[t-1],t}\right)$ is affected by dispatch decisions, the decision-dependency coefficient $\boldsymbol{\lambda}^{cov}_d$ becomes a matrix with the special structure in (3c).

2.2.2 *Data-Driven Method for Obtaining Decision-Dependent Coefficients*

The values of λ^{μ}_d and $\boldsymbol{\lambda}^{cov}_d$ are the most important in the decision-dependent ambiguity sets since they directly determine how the dispatch decisions affects the values of mean vector $\boldsymbol{\mu}\left(\boldsymbol{d}^s_{[t-1],t}\right)$ and covariance matrix $\Sigma\left(\boldsymbol{d}^s_{[t-1],t}\right)$. In this subsection, a data-driven approach is provided based on real-world data to obtain the two parameters. Assuming there are N historical data samples, each sample $a = 1, ..., N$ contains the data of demand shifting $d^s_{d,\tau,t,a}$ and uncertainty realization $\boldsymbol{\xi}_a$. Since λ^{μ}_d and $\boldsymbol{\lambda}^{cov}_d$ in (3a)-(3b) can be obtained once $\hat{\mu}_d$, μ_d, $\hat{\Sigma}_d$, Σ_d and $\sum\limits_{\tau=1}^{t-1} d^s_{d,\tau,t}$ are known, the following steps are offered to calculate λ^{μ}_d and $\boldsymbol{\lambda}^{cov}_d$.

First, it should be noted that there are many different values of $\sum\limits_{\tau=1}^{t-1} d^s_{d,\tau,t,a}$ in sample data, but only one certain value is used in (3a) to calculate λ^{μ}_d. To this end, the DBSCAN clustering method [24] with given radius and number of minimal points is adopted to divide the N samples into M clusters based on the value of $\sum\limits_{\tau=1}^{t-1} d^s_{d,\tau,t,a}$. Then the K-means clustering method is applied to find the center point $\sum\limits_{\tau=1}^{t-1} d^{s,cen}_{d,\tau,t,b}$ in each cluster $b = 1, ..., M$, which will be regarded as the value of $\sum\limits_{\tau=1}^{t-1} d^s_{d,\tau,t}$ in cluster b. With that, each cluster has a certain number of samples and a unique value of $\sum\limits_{\tau=1}^{t-1} d^s_{d,\tau,t}$ (equal to $\sum\limits_{\tau=1}^{t-1} d^{s,cen}_{d,\tau,t,b}$). Then the four parameters $\hat{\mu}_{d,b}$, $\mu_{d,b}$, $\hat{\Sigma}_{d,b}$, $\Sigma_{d,b}$ and the value of $\lambda^{\mu}_{d,b}$ can be calculated by using the sample data in cluster b. With these, the value of λ^{μ}_d is calculated by the weighted average as

$$\lambda^u_d = \sum_{b=1}^{M} \frac{N_b}{N} \lambda^u_{d,b} \tag{3d}$$

where N_b is the number of samples in cluster b.

Similarly, the diagonal elements and a part of non-diagonal elements in $\boldsymbol{\lambda}^{cov}_d$ can be calculated by the same way of calculating λ^{μ}_d. While for the rest part of non-diagonal elements (in Example 1, they are $\lambda^{cov}_{1,12}$, $\lambda^{cov}_{1,21}$,$\lambda^{cov}_{2,12}$, $\lambda^{cov}_{2,21}$), we take Example 1 for explanation. Specifically, the value of the element in first row and second column of $\boldsymbol{\lambda}^{cov}_d$ in cluster b can be calculated by

$$(\Sigma)_{12,b} = \left(\hat{\Sigma}\right)_{12,b} + \sum_{\tau=1}^{t-1} \lambda^{cov}_{1,12,b} d^s_{1,\tau,t,b} + \sum_{\tau=1}^{t-1} \lambda^{cov}_{2,12,b} d^s_{2,\tau,t,b} \tag{3e}$$

where $(\Sigma)_{12,b}$ and $\left(\hat{\Sigma}\right)_{12,b}$ represents the element in first row and second column of the two matrices.

Note that the equation (3e) has two unknowns $\lambda^{cov}_{1,12,b}$ and $\lambda^{cov}_{2,12,b}$, and thus the equation cannot be directly solved if only one cluster is used. To this end, we adopt DBSCAN and K-means clusting methods again to divide the cluster b into several sub-clusters and find the center points of these sub-clusters. The number of sub-clusters is equal to the number of deferrable loads. In Example 1, we divide cluster b into two sub-cluster as $c^{sub}_{b,1}$ and $c^{sub}_{b,2}$. The two sub-clusters are assumed to have the same values of $\lambda^{cov}_{1,12,b}$ and $\lambda^{cov}_{2,12,b}$. Then the equation (3e) becomes

$$\begin{cases} (\Sigma)_{12,b^{sub}_{a,1}} = \left(\hat{\Sigma}\right)_{12,b^{sub}_{a,1}} + \sum\limits_{\tau=1}^{t-1} \lambda^{cov}_{1,12,a} d^s_{1,\tau,t,b^{sub}_{a,1}} \\ \qquad\qquad + \sum\limits_{\tau=1}^{t-1} \lambda^{cov}_{2,12,a} d^s_{2,\tau,t,b^{sub}_{a,1}} \\ (\Sigma)_{12,b^{sub}_{a,2}} = \left(\hat{\Sigma}\right)_{12,b^{sub}_{a,2}} + \sum\limits_{\tau=1}^{t-1} \lambda^{cov}_{1,12,a} d^s_{1,\tau,t,b^{sub}_{a,2}} \\ \qquad\qquad + \sum\limits_{\tau=1}^{t-1} \lambda^{cov}_{2,12,a} d^s_{2,\tau,t,b^{sub}_{a,2}} \end{cases} \tag{3f}$$

Equation (3f) contains two equations and two unknowns. By solving it, we can obtain the values of $\lambda^{cov}_{1,12,b}$ and $\lambda^{cov}_{2,12,b}$ in cluster b. Other non-diagonal elements $\lambda^{cov}_{1,21,b}$ and $\lambda^{cov}_{2,21,b}$ are calculated by the same way. After iterating through all clusters, the values of these non-diagonal elements in $\boldsymbol{\lambda}^{cov}_d$ can be calculated by weighted average like (3d).

2.3 *Multistage Distributionally Robust Generation Dispatch Model with Decision-Dependent Ambiguity Set*

The proposed multistage distributionally robust generation dispatch model sequentially makes decisions considering the worst-case probability distribution lying in the decision-dependent ambiguity set. Considering the dynamic decision-making process stated in Fig. 1, the proposed multistage DRO model is written in a nested optimization structure as follows

$$\min_{(\boldsymbol{x}_0,\boldsymbol{y}_0)\in\mathcal{X}_0}\left\{f\left(\boldsymbol{x}_0,\boldsymbol{y}_0\right)+\max_{\mathbb{P}_1\in\mathcal{P}_1}\mathbb{E}_{\mathbb{P}_1}\left[\min_{(\boldsymbol{x}_1,\boldsymbol{y}_1)\in\mathcal{X}_1(\boldsymbol{x}_0,\boldsymbol{\xi}_1)} g_1\left(\boldsymbol{x}_1,\boldsymbol{y}_1\right)\right.\right.$$
$$+\max_{\mathbb{P}_2\in\mathcal{P}_2\left(\boldsymbol{x}_{[1]}\right)}\mathbb{E}_{\mathbb{P}_2}\left[\min_{(\boldsymbol{x}_2,\boldsymbol{y}_2)\in\mathcal{X}_2(\boldsymbol{x}_0,\boldsymbol{x}_1,\boldsymbol{\xi}_2)} g_2\left(\boldsymbol{x}_2,\boldsymbol{y}_2\right)+\cdots\right.$$
$$+\max_{\mathbb{P}_t\in\mathcal{P}_t\left(\boldsymbol{x}_{[t-1]}\right)}\mathbb{E}_{\mathbb{P}_t}\left[\min_{(\boldsymbol{x}_t,\boldsymbol{y}_t)\in\mathcal{X}_t\left(\boldsymbol{x}_0,\boldsymbol{x}_{[t-1]},\boldsymbol{\xi}_t\right)} g_t\left(\boldsymbol{x}_t,\boldsymbol{y}_t\right)+\cdots\right.$$
$$\left.\left.\left.\left.\left.+\max_{\mathbb{P}_T\in\mathcal{P}_T\left(\boldsymbol{x}_{[T-1]}\right)}\mathbb{E}_{\mathbb{P}_T}\min_{\boldsymbol{y}_T\in\mathcal{X}_T\left(\boldsymbol{x}_0,\boldsymbol{x}_{[T-1]},\boldsymbol{\xi}_T\right)} g_T\left(\boldsymbol{y}_T\right)\right]\right]\right]\right\}\tag{4a}$$

where

$$\begin{cases}\boldsymbol{x}_0=\left\{p_{i,t},r_{i,t}^{\pm}\right\},\boldsymbol{y}_0=\left\{\hat{w}_{h,t}\right\}\\ \boldsymbol{x}_t=\left\{d_{m,t,\tau}^{s},\forall t\in\mathcal{T}/\{T\}\right.,\left.\forall\tau=t+1,...,T\right\}\\ \boldsymbol{y}_t=\left\{p_{i,t}^{\pm},w_{h,t},d_{n,t}^{c},d_{m,t}^{s,ls},d_{n,t}^{r,ls}\right\}\end{cases}\tag{4b}$$

$$f\left(\boldsymbol{x}_0,\boldsymbol{y}_0\right)=\sum_{t\in\mathcal{T}}\sum_{i\in\mathcal{G}}\left(\alpha_i p_{i,t}+\beta_i^{+}r_{i,t}^{+}+\beta_i^{-}r_{i,t}^{-}\right)\tag{4c}$$

$$\begin{aligned}&g_t\left(\boldsymbol{x}_t,\boldsymbol{y}_t\right)=\\&\sum_{t\in\mathcal{T}}\sum_{i\in\mathcal{G}}\left(d_i^{+}p_{i,t}^{+}+d_i^{-}p_{i,t}^{-}\right)+\sum_{t\in\mathcal{T}}\sum_{n\in\mathcal{D}_r}\left(c^{ls}d_{n,t}^{r,ls}+c_n^{c}d_{n,t}^{c}\right)\\&\quad+\sum_{t\in\mathcal{T}}\sum_{m\in\mathcal{D}_s}\left(c^{ls}d_{m,t}^{s,ls}+\sum_{\tau=t+1}^{T}c_m^{s}d_{m,t,\tau}^{s}\right)\end{aligned}\tag{4d}$$

Equation (4a) presents the nested objective function of the multistage DRO model where the probability distribution of random variables is dependent to the previous stages' dispatch decisions. In (4b), $\boldsymbol{x}_0$ and $\boldsymbol{x}_t$ denote state variables connecting different stages, $\boldsymbol{y}_0$ and $\boldsymbol{y}_t$ are stage variables which only appear at the corresponding stages. The pre-dispatch stage minimizes generation and reserve cost of thermal generators (4c), and re-dispatch stage minimizes the sum of up- and down-regulation cost, demand shifting cost, demand curtailment cost, and load shedding penalty cost (4d).

The feasible region of pre-dispatch variables and re-dispatch variables are given by

$$\mathcal{X}_0=\{\,(\boldsymbol{x}_0,\boldsymbol{y}_0)|$$

$$\sum_{i\in\mathcal{G}}p_{i,t}+\sum_{h\in\mathcal{W}}\hat{w}_{h,t}=\sum_{m\in\mathcal{D}_s}D_{m,t}^{s,f}+\sum_{n\in\mathcal{D}_r}D_{n,t}^{r,f},\forall t\in\mathcal{T}\tag{5a}$$

$$\begin{aligned}-F_l\leq&\sum_{i\in\mathcal{G}}\pi_{il}p_{i,t}+\sum_{h\in\mathcal{W}}\pi_{hl}\hat{w}_{h,t}-\sum_{m\in\mathcal{D}_s}\pi_{ml}D_{m,t}^{s,f}\\&-\sum_{n\in\mathcal{D}_r}\pi_{nl}D_{n,t}^{r,f}\leq F_l,\forall l\in\mathcal{L},\forall t\in\mathcal{T}\end{aligned}\tag{5b}$$

$$-\mathcal{R}_i^{d}\leq\left(p_{i,t}+r_{i,t}^{+}\right)-\left(p_{i,t-1}-r_{i,t-1}^{-}\right)\leq\mathcal{R}_i^{u},\forall i\in\mathcal{G},\forall t\in\mathcal{T}\tag{5c}$$

$$-\mathcal{R}_i^{d}\leq\left(p_{i,t}-r_{i,t}^{-}\right)-\left(p_{i,t-1}+r_{i,t-1}^{+}\right)\leq\mathcal{R}_i^{u},\forall i\in\mathcal{G},\forall t\in\mathcal{T}\tag{5d}$$

$$0\leq r_{i,t}^{-}\leq\mathcal{R}_i^{d},0\leq r_{i,t}^{+}\leq\mathcal{R}_i^{u},\forall i\in\mathcal{G},\forall t\in\mathcal{T}\tag{5e}$$

$$P_i^{l}\leq p_{i,t}-r_{i,t}^{-},p_{i,t}+r_{i,t}^{+}\leq P_i^{u},\forall i\in\mathcal{G},\forall t\in\mathcal{T}\tag{5f}$$

$$0\leq\hat{w}_{h,t}\leq w_{h,t}^{f},\forall h\in\mathcal{W},\forall t\in\mathcal{T}\}\tag{5g}$$

and

$$\mathcal{X}_t=\{\,(\boldsymbol{x}_t,\boldsymbol{y}_t)|$$

$$0\leq p_{i,t}^{-}\leq r_{i,t}^{-},0\leq p_{i,t}^{+}\leq r_{i,t}^{+},\forall i\in\mathcal{G},\forall t\in\mathcal{T}\tag{6a}$$

$$\begin{aligned}&\sum_{i\in\mathcal{G}}\left(p_{i,t}+p_{i,t}^{+}-p_{i,t}^{-}\right)+\sum_{h\in\mathcal{W}}w_{h,t}\\&\quad=\sum_{m\in\mathcal{D}_s}\left(D_{m,t}^{s}-d_{m,t}^{s,ls}-\sum_{\tau=t+1}^{T}d_{m,t,\tau}^{s}\right)\\&\qquad+\sum_{n\in\mathcal{D}_r}\left(D_{n,t}^{r}-d_{m,t}^{r,ls}-d_{m,t}^{c}\right),\forall t\in\mathcal{T}\end{aligned}\tag{6b}$$

$$\begin{aligned}-F_l\leq&\sum_{i\in\mathcal{G}}\pi_{il}\left(p_{i,t}+p_{i,t}^{+}-p_{i,t}^{-}\right)+\sum_{h\in\mathcal{W}}\pi_{hl}w_{h,t}\\&-\sum_{m\in\mathcal{D}_s}\pi_{ml}\left(D_{m,t}^{s}-d_{m,t}^{s,ls}-\sum_{\tau=t+1}^{T}d_{m,t,\tau}^{s}\right)\\&-\sum_{n\in\mathcal{D}_r}\pi_{nl}\left(D_{n,t}^{r}-d_{m,t}^{r,ls}-d_{m,t}^{c}\right)\leq F_l,\forall l\in\mathcal{L},\forall t\in\mathcal{T}\end{aligned}\tag{6c}$$

$$\begin{cases}0\leq d_{m,t}^{s,ls}+d_{m,t,\tau}^{s}\leq D_{m,t}^{s},\forall m\in\mathcal{D}_s,\forall t\in\mathcal{T}\\0\leq d_{m,t,\tau}^{s}\leq d_{m,t,\tau}^{s,u},\forall m\in\mathcal{D}_s,\forall t\in\mathcal{T}/\{T\},\forall\tau=t+1,...,T\end{cases}\tag{6d}$$

$$\begin{cases}0\leq d_{n,t}^{r,ls}+d_{n,t}^{c}\leq D_{n,t}^{r}\\0\leq d_{n,t}^{c}\leq d_{n,t}^{c,u}\end{cases},\forall n\in\mathcal{D}_r,\forall t\in\mathcal{T}\tag{6e}$$

$$0\leq w_{h,t}\leq w_{h,t}^{o},\forall h\in\mathcal{W},\forall t\in\mathcal{T}\}\tag{6f}$$

Constraints (5a) and (5b) state the power balance equation and power flow limits. The ramping restrictions of generators when offering the reserve capacities are given in (5c) and (5d). Constraints (5e) and (5f) limit the reserve capacities and the upper and lower bounds of generator output considering reserve requirements, respectively. Constraint (5g) restricts the scheduled wind power based on the forecast output. Load shedding is not allowed in pre-dispatch stage.

Constraint (6a) restricts the up- and down-regulation power of generators within reserve capacities. Power balance and power flow limits are stated in (6b) and (6c). Constraint (6d) and (6e) present the upper bounds of demand shifting, demand curtailment and load shedding. Constraint (6f) allows wind power curtailment in re-dispatch stage.

3 Solution Methodology

The proposed multistage DRO model is difficult to solve due to the nested optimization structure and decision-dependent ambiguity set. In this section, the original model is first reformulated into a tractable form, then an improved SDDiP algorithm is developed to handle the model.

3.1 Model Reformulation

The proposed multistage DRO model can be written in a dynamic programming form. The equivalent recursion of objective function (4a) is written as the following Bellman equation.

For the pre-dispatch stage, one has

$$\begin{aligned}&Q_0 = \min\left\{f\left(\boldsymbol{x}_0,\boldsymbol{y}_0\right)+\max_{\mathbb{P}_1\in\mathcal{P}_1}\mathbb{E}_{\mathbb{P}_1}\left[Q_1\left(\boldsymbol{x}_0,\boldsymbol{\xi}_1\right)\right]\right\}\\&\text{s.t. } \boldsymbol{x}_0,\boldsymbol{y}_0\in\mathcal{X}_0\end{aligned}\tag{7a}$$

where the ambiguity set $\mathcal{P}_1$ is decision-independent since there is no demand shifting decision in the pre-dispatch stage.

For the re-dispatch stages, one has

$$\begin{aligned}&Q_t\left(\boldsymbol{x}_0,\boldsymbol{x}_{[t-1]},\boldsymbol{\xi}_t\right)=\\&\min\left\{\begin{aligned}&g_t\left(\boldsymbol{x}_t,\boldsymbol{y}_t\right)+\\&\max_{\mathbb{P}_{t+1}\in\mathcal{P}_{t+1}\left(\boldsymbol{x}_{[t]}\right)}\mathbb{E}_{\mathbb{P}_{t+1}}\left[Q_{t+1}\left(\boldsymbol{x}_0,\boldsymbol{x}_{[t]},\boldsymbol{\xi}_{t+1}\right)\right]\end{aligned}\right\}\\&\text{s.t. } \boldsymbol{x}_t,\boldsymbol{y}_t\in\mathcal{X}_t\left(\boldsymbol{x}_0,\boldsymbol{x}_{[t-1]},\boldsymbol{\xi}_t\right)\end{aligned}\tag{7b}$$

where we set $Q_{t+1}\left(\boldsymbol{x}_0,\boldsymbol{x}_{[t]},\boldsymbol{\xi}_{t+1}\right)\equiv 0$

The continuous probability distribution in the ambiguity set is discretized by N_{t+1} realizations. Then the inner maximization problem of Bellman equations is stated as follows

$$\max_{p_r\in\mathcal{P}_{t+1}\left(\boldsymbol{x}_{[t]}\right)}\sum_{r=1}^{N_{t+1}}p_rQ_{r,t+1}\left(\boldsymbol{x}_0,\boldsymbol{x}_{[t]},\boldsymbol{\xi}_{r,t+1}\right)\tag{8a}$$

$$\begin{aligned}&\text{s.t. } \mathcal{P}_{t+1}\left(\boldsymbol{x}_{[t]}\right)=\\&\left\{p_r\left|\begin{aligned}&\sum_{r=1}^{N_{t+1}}p_r=1:\gamma\\&\sum_{r=1}^{N_{t+1}}p_r\boldsymbol{\xi}_{r,t+1}=\boldsymbol{\mu}\left(\boldsymbol{x}_{[t]}\right):\boldsymbol{\varphi}\\&\sum_{r=1}^{N_{t+1}}p_r\left[\left(\boldsymbol{\xi}_{r,t+1}-\boldsymbol{\mu}\left(\boldsymbol{x}_{[t]}\right)\right)\left(\boldsymbol{\xi}_{r,t+1}-\boldsymbol{\mu}\left(\boldsymbol{x}_{[t]}\right)\right)^{\mathrm{T}}\right]\\&\qquad=\Sigma\left(\boldsymbol{x}_{[t]}\right):\boldsymbol{\psi}\end{aligned}\right.\right.\end{aligned}\tag{8b}$$

By dualizing the problem (8) and combining it with the outer minimization problem of (7), the pre-dispatch and re-dispatch problems are recast as

$$\begin{aligned}&Q_0=\min f\left(\boldsymbol{x}_0,\boldsymbol{y}_0\right)+\gamma+\boldsymbol{\varphi}^{\mathrm{T}}\hat{\boldsymbol{\mu}}+\left\langle\hat{\Sigma},\boldsymbol{\psi}\right\rangle_{\mathrm{F}}\\&\text{s.t. } \boldsymbol{x}_0,\boldsymbol{y}_0\in\mathcal{X}_0\\&\quad\gamma+\boldsymbol{\varphi}^{\mathrm{T}}\boldsymbol{\xi}_{r,1}+\left\langle\left(\boldsymbol{\xi}_{r,1}-\hat{\boldsymbol{\mu}}\right)\left(\boldsymbol{\xi}_{r,1}-\hat{\boldsymbol{\mu}}\right)^{\mathrm{T}},\boldsymbol{\psi}\right\rangle_{\mathrm{F}}\\&\qquad\geq Q_{r,1},\forall r\in[N_1]\end{aligned}\tag{9a}$$

$$\begin{aligned}&Q_t=\min g_t\left(\boldsymbol{x}_t,\boldsymbol{y}_t\right)+\gamma+\boldsymbol{\varphi}^{\mathrm{T}}\boldsymbol{\mu}\left(\boldsymbol{x}_{[t]}\right)+\left\langle\Sigma\left(\boldsymbol{x}_{[t]}\right),\boldsymbol{\psi}\right\rangle_{\mathrm{F}}\\&\text{s.t. } \boldsymbol{x}_t,\boldsymbol{y}_t\in\mathcal{X}_t\left(\boldsymbol{x}_0,\boldsymbol{x}_{[t-1]},\boldsymbol{\xi}_t\right)\\&\gamma+\boldsymbol{\varphi}^{\mathrm{T}}\boldsymbol{\xi}_{r,t+1}\\&\quad+\left\langle\left[\left(\boldsymbol{\xi}_{r,t+1}-\boldsymbol{\mu}\left(\boldsymbol{x}_{[t]}\right)\right)\left(\boldsymbol{\xi}_{r,t+1}-\boldsymbol{\mu}\left(\boldsymbol{x}_{[t]}\right)\right)^{\mathrm{T}}\right],\boldsymbol{\psi}\right\rangle_{\mathrm{F}}\\&\qquad\geq Q_{r,t+1},\forall r\in[N_{t+1}]\end{aligned}\tag{9b}$$

where $\langle\boldsymbol{A},\boldsymbol{B}\rangle_{\mathrm{F}}$ denotes the Frobenius inner product of matrix $\boldsymbol{A}$ and $\boldsymbol{B}$.

Problems (9a)-(9b) eliminate the variable p_r while retains the decision-dependent probability distribution information via dual variables. However, the following bilinear terms and trilinear terms occur in the objective function and constraints when substitute (3) into (9b)

$$\boldsymbol{\varphi}^{\mathrm{T}}\boldsymbol{\mu}\left(\boldsymbol{x}_{[t]}\right)=\sum_{j\in\mathcal{D}_r\cup\mathcal{W}}\hat{\mu}_j\varphi_j+\sum_{d\in\mathcal{D}_s}\hat{\mu}_d\varphi_d\left(1+\sum_{\tau=1}^{t}\lambda_d^{\mu}d_{d,\tau,t+1}^{s}\right)\tag{10a}$$

$$\left\langle\Sigma\left(\boldsymbol{x}_{[t]}\right),\boldsymbol{\psi}\right\rangle_{\mathrm{F}}=\left\langle\hat{\Sigma},\boldsymbol{\psi}\right\rangle_{\mathrm{F}}+\sum_{d\in\mathcal{D}_s}\sum_{\tau=1}^{t}d_{d,\tau,t+1}^{s}\langle\boldsymbol{\lambda}_d^{cov},\boldsymbol{\psi}\rangle_{\mathrm{F}}\tag{10b}$$

$$\begin{aligned}&\left\langle\boldsymbol{\xi}_{r,t+1}\boldsymbol{\mu}\left(\boldsymbol{x}_{[t]}\right)^{\mathrm{T}},\boldsymbol{\psi}\right\rangle_{\mathrm{F}}=\sum_{v\in\mathcal{U}}\sum_{v'\in\mathcal{U}}\xi_{v,r,t+1}\hat{\mu}_{v'}\psi_{v,v'}\\&\qquad+\sum_{v\in\mathcal{U}}\sum_{d\in\mathcal{D}_s}\left(\xi_{v,r,t+1}\hat{\mu}_d\psi_{v,d}\sum_{\tau=1}^{t}\lambda_d^{\mu}d_{d,\tau,t+1}^{s}\right)\end{aligned}\tag{10c}$$

$$\begin{aligned}&\left\langle\boldsymbol{\mu}\left(\boldsymbol{x}_{[t]}\right)\boldsymbol{\mu}\left(\boldsymbol{x}_{[t]}\right)^{T},\boldsymbol{\psi}\right\rangle_{\mathrm{F}}=\sum_{v\in\mathcal{U}}\sum_{v'\in\mathcal{U}}\hat{\mu}_v\hat{\mu}_{v'}\psi_{v,v'}\\&+\sum_{d\in\mathcal{D}_s}\sum_{v\in\mathcal{U}}\left(\hat{\mu}_d\hat{\mu}_v\psi_{d,v}\sum_{\tau=1}^{t}\lambda_d^{\mu}d_{d,\tau,t+1}^{s}\right)\\&+\sum_{v\in\mathcal{U}}\sum_{d\in\mathcal{D}_s}\left(\hat{\mu}_v\hat{\mu}_d\psi_{v,d}\sum_{\tau=1}^{t}\lambda_d^{\mu}d_{d,\tau,t+1}^{s}\right)\\&+\sum_{d\in\mathcal{D}_s}\sum_{d'\in\mathcal{D}_s}\left(\hat{\mu}_d\hat{\mu}_{d'}\psi_{d,d'}\sum_{\tau=1}^{t}\lambda_d^{\mu}d_{d,\tau,t+1}^{s}\sum_{\tau'=1}^{t}\lambda_{d'}^{\mu}d_{d',\tau',t+1}^{s}\right)\end{aligned}\tag{10d}$$

These bilinear and trilinear terms are the multiplication of two and three continuous variables. The basic idea of linearization is to employ binary expansion to discretize state variables $\boldsymbol{x}_0$ and $\boldsymbol{x}_t$. After that, the bilinear and trilinear terms contain one or two binary variables and only one continuous variable, which can be further transformed into linear terms by using McCormick envelopes. The binary expansion is stated as follows

$$p_{it}=P_i^l+\Delta p_i\sum_{k=0}^{K_0}2^kz_{k,i,t}^{p},\text{ where }\Delta p_i=\frac{P_i^u-P_i^l}{2^{K_0}}\tag{11a}$$

$$r_{it}^{+/-}=\Delta r_i^{+/-}\sum_{k=0}^{K_0}2^kz_{k,i,t}^{ru/rd},\text{ where }\Delta r_i^{+/-}=\frac{\mathcal{R}_i^{u/d}}{2^{K_0}}\tag{11b}$$

$$d_{d,t,\tau}^{s}=\Delta d_{d,t,\tau}\sum_{k=0}^{K}2^kz_{k,d,t,\tau}^{d},\text{ where }\Delta d_{d,t,\tau}=\frac{d_{d,t,\tau}^{s,u}}{2^{K}}\tag{11c}$$

$$
\begin{aligned}
&\gamma+\boldsymbol{\varphi}^{\mathrm{T}}\boldsymbol{\xi}_{r,t+1}+\left\langle\boldsymbol{\xi}_{r,t+1}\boldsymbol{\xi}_{r,t+1}^{\mathrm{T}},\boldsymbol{\psi}\right\rangle_{\mathrm{F}}-\sum_{v\in\mathcal{U}}\sum_{v'\in\mathcal{U}}\xi_{v,r,t+1}\hat{\mu}_{v'}\left(\psi_{v,v'}+\psi_{v',v}\right)\\
&-\sum_{d\in\mathcal{D}_s}\sum_{v\in\mathcal{U}}\sum_{\tau=1}^{t}\sum_{k=0}^{K}2^k\Delta d_{d,\tau,t+1}\hat{\mu}_d\xi_{v,r,t+1}\lambda_d^{\mu}\left(\delta_{k,d,v,\tau,t+1}+\delta'_{k,v,d,\tau,t+1}\right)\\
&+\sum_{v\in\mathcal{U}}\sum_{v'\in\mathcal{U}}\hat{\mu}_v\hat{\mu}_{v'}\psi_{v,v'}+\sum_{d\in\mathcal{D}_s}\sum_{v\in\mathcal{U}}\sum_{\tau=1}^{t}\sum_{k=0}^{K}2^k\Delta d_{d,\tau,t+1}\hat{\mu}_d\hat{\mu}_v\lambda_d^{\mu}\left(\delta_{k,d,v,\tau,t+1}+\delta'_{k,v,d,\tau,t+1}\right)\\
&+\sum_{d\in\mathcal{D}_s}\sum_{d'\in\mathcal{D}_s}\sum_{\tau=1}^{t}\sum_{\tau'=1}^{t}\sum_{k=0}^{K}\sum_{k'=0}^{K}\left(2^{k+k'}\Delta d_{d,\tau,t+1}\Delta d_{d',\tau',t+1}\hat{\mu}_d\hat{\mu}_{d'}\lambda_d^{\mu}\lambda_{d'}^{\mu}\varpi_{k,k',d,d',\tau,\tau',t+1}\right)\geq Q_{r,t+1},\forall r\in[N_{t+1}]
\end{aligned}
\tag{13d}
$$

Then the bilinear and trilinear terms are represented as (12) by using McCormick envelopes $\mathcal{M}$

$$
\begin{cases}
\sigma_{k,d,\tau,t+1}\in\mathcal{M}\left(\varphi_d z_{k,d,\tau,t+1}^d\right)\\
\varepsilon_{k,d,v,v',\tau,t+1}\in\mathcal{M}\left(\psi_{v,v'}z_{k,d,\tau,t+1}^d\right)\\
\delta_{k,d,v,\tau,t+1}\in\mathcal{M}\left(\psi_{d,v}z_{k,d,\tau,t+1}^d\right)\\
\delta'_{k,v,d,\tau,t+1}\in\mathcal{M}\left(\psi_{v,d}z_{k,d,\tau,t+1}^d\right)\\
\varpi_{k,k',d,d',\tau,\tau',t+1}\in\mathcal{M}\left(\psi_{d,d'}z_{k,d,\tau,t+1}^d z_{k',d',\tau',t+1}^d\right)
\end{cases}
\tag{12}
$$

With (11a)-(11c) and (12), the Bellman equations are finally reformulated as (13a)-(13d)

$$
\begin{aligned}
Q_t=&\min g_t\left(\boldsymbol{x}_t,\boldsymbol{y}_t\right)+\gamma+\sum_{v\in\mathcal{U}}\hat{\mu}_v\lambda_v+\sum_{v\in\mathcal{U}}\sum_{v'\in\mathcal{U}}\hat{\Sigma}_{v,v'}\psi_{v,v'}\\
&+\sum_{d\in\mathcal{D}_s}\sum_{\tau=1}^{t}\sum_{k=0}^{K}2^k\Delta d_{d,\tau,t+1}\hat{\mu}_d\lambda_d^{\mu}\sigma_{k,d,\tau,t+1}\\
&+\sum_{d\in\mathcal{D}_s}\sum_{v\in\mathcal{U}}\sum_{v'\in\mathcal{U}}\sum_{\tau=1}^{t}\sum_{k=0}^{K}2^k\Delta d_{d,\tau,t+1}\lambda_{d,v,v'}^{cov}\varepsilon_{k,d,v,v',\tau,t+1}
\end{aligned}
\tag{13a}
$$

$$
\text{s.t.}\quad \text{(11a)-(11c)},\ (12) \tag{13b}
$$

$$
\boldsymbol{x}_t,\boldsymbol{y}_t\in\mathcal{X}_t\left(\boldsymbol{x}_0,\boldsymbol{x}_{[t-1]},\boldsymbol{\xi}_t\right) \tag{13c}
$$

3.2 Improved SDDiP Algorithm

The standard SDDiP algorithm requires that the stage variables only connect consecutive two stages [25]. That is, the Bellman equation at stage t depends only on the stage variables at stage $t-1$. However, the proposed model at stage t depends on not only the pre-dispatch variables $\boldsymbol{x}_0$, but also the demand shifting decisions $\boldsymbol{x}_{[t-1]}$ at re-dispatch stages $1,\ldots,t-1$. Thus, the standard SDDiP cannot be employed directly to handle the multistage DRO model with cross-time state variables. In this section, we improved standard SDDiP by introducing dummy variables into Bellman equations. The dummy variables copy the stage variables that are not used at previous stages, which will be passed to the subsequent stages until the stage variables are utilized. In other words, the dummy variables make the unused stage variables at stages $1,\ldots,t-2$ become the variables at stage $t-1$ by copying and passing them. In this way, the Bellman equation at stage t depends only on the stage variables at stage $t-1$, which enables SDDiP to be employed.

Specifically, the re-dispatch problem with dummy variables for stage 1 is formulated as

$$
\begin{aligned}
&Q_1=\min g_1\left(\boldsymbol{x}_1,\boldsymbol{y}_1\right)+\gamma+\boldsymbol{\varphi}^{\mathrm{T}}\boldsymbol{\mu}\left(\boldsymbol{x}_1\right)+\left\langle\Sigma\left(\boldsymbol{x}_1\right),\boldsymbol{\psi}\right\rangle_{\mathrm{F}}\\
&\text{s.t.}\quad \text{(11a)}-\text{(11c)},\ (12),\ \text{(13d)}\\
&\qquad \boldsymbol{x}_1,\boldsymbol{y}_1\in\mathcal{X}_1\left(\boldsymbol{z}_0^g,\boldsymbol{\xi}_1\right)\\
&\qquad \boldsymbol{z}_1^{g,copy}=M_1\boldsymbol{z}_0^g
\end{aligned}
\tag{14a}
$$

where $\boldsymbol{z}_0^g=\left\{z_{k,i,t}^p,z_{k,i,t}^{ru},z_{k,i,t}^{rd}\right\}$ denotes the binary pre-dispatch state variables in (11). M_1 is the coefficient matrix that selects certain variables of $\boldsymbol{z}_0^g$. $\boldsymbol{z}_1^{g,copy}$ denotes the dummy stage variables that copy the pre-dispatch stage variables for stages $2,\ldots,T$. That means only $\left\{z_{k,i,1}^p,z_{k,i,1}^{ru},z_{k,i,1}^{rd}\right\}$ are utilized in problem Q_1, while $\left\{z_{k,i,t}^p,z_{k,i,t}^{ru},z_{k,i,t}^{rd},\forall t=2,...,T\right\}$ are copied by $\boldsymbol{z}_1^{g,copy}$ and passed to subsequent stages.

Similarly, the re-dispatch problems with dummy variables for stage $t=2,...,T-1$ and T are formulated as

$$
\begin{aligned}
&Q_t=\min g_t\left(\boldsymbol{x}_t,\boldsymbol{y}_t\right)+\gamma+\boldsymbol{\varphi}^{\mathrm{T}}\boldsymbol{\mu}\left(\boldsymbol{z}_{t-1}^{d,copy},\boldsymbol{z}_{t-1}^d,\boldsymbol{x}_t\right)\\
&\quad+\left\langle\Sigma\left(\boldsymbol{z}_{t-1}^{d,copy},\boldsymbol{z}_{t-1}^d,\boldsymbol{x}_t\right),\boldsymbol{\psi}\right\rangle_{\mathrm{F}}\\
&\text{s.t.}\quad \text{(11a)}-\text{(11c)},(12),\text{(13d)}\\
&\qquad \boldsymbol{x}_t,\boldsymbol{y}_t\in\mathcal{X}_t\left(\boldsymbol{z}_{t-1}^{g,copy},\boldsymbol{z}_{t-1}^{d,copy},\boldsymbol{z}_{t-1}^d,\boldsymbol{\xi}_t\right)\\
&\qquad \boldsymbol{z}_t^{g,copy}=M_t\boldsymbol{z}_{t-1}^{g,copy}\\
&\qquad \boldsymbol{z}_t^{d,copy}=\begin{bmatrix}G_t\boldsymbol{z}_{t-1}^d\\ L_t\boldsymbol{z}_{t-1}^{d,copy}\end{bmatrix}
\end{aligned}
\tag{14b}
$$

$$
\begin{aligned}
&Q_T=\min g_T\left(\boldsymbol{y}_T\right)\\
&\text{s.t.}\quad \text{(11a)}-\text{(11c)}\\
&\qquad \boldsymbol{y}_T\in\mathcal{X}_T\left(\boldsymbol{z}_{T-1}^{g,copy},\boldsymbol{z}_{T-1}^{d,copy},\boldsymbol{\xi}_T\right)
\end{aligned}
\tag{14c}
$$

where $\boldsymbol{z}_t^d=\left\{z_{k,d,t,\tau}^d,\forall\tau=t+1,...,T\right\}$ denotes the binary demand shifting variables at stage t. Since the problem Q_t is only affected by $\left\{z_{k,d,\tau,t}^d,\forall\tau=1,...,t-1\right\}$, the unused variables $\left\{z_{k,d,\tau_1,\tau_2}^d,\forall\tau_1=1,...,t-1,\forall\tau_2=t+2,...,T\right\}$ are copied by the dummy variable $\boldsymbol{z}_t^{d,copy}$. G_t and L_t are coefficient matrices. $G_t\boldsymbol{z}_{t-1}^d=\left\{z_{k,d,t-1,\tau}^d,\forall\tau=t+2,...,T\right\}$ and $L_t\boldsymbol{z}_{t-1}^{d,copy}=\left\{z_{k,d,t-1,\tau}^{d,copy},\forall\tau=t+2,...,T\right\}$ selects the unused part of variables $\boldsymbol{z}_{t-1}^d$ and $\boldsymbol{z}_{t-1}^{d,copy}$, respectively. Note that $\boldsymbol{z}_1^{d,copy}$ does not exist in Q_1, thus the variable $\boldsymbol{z}_2^{d,copy}$ in Q_2 is expressed as $G_t\boldsymbol{z}_1^d$.

After replacing cross-time stage variables $\boldsymbol{z}_0^g$ and $\boldsymbol{z}_{[t-2]}^d$ in (13) with dummy variables $\boldsymbol{z}_{t-1}^{g,copy}$ and $\boldsymbol{z}_{t-1}^{d,copy}$, the problem Q_t

depends only on the variables at stage $t-1$. Thus, SDDiP can be deployed with the following forward and backward steps.

(1) Forward Step

The forward step is to obtain the optimal solution under the given uncertainty path, where the value function $Q_{r,t+1}$ in (13d) is replaced by its under-approximation cutting planes $\mathcal{V}^{\ell}_{r,t}$. For the problem Q_0 and Q_t, the cutting planes are

$$\mathcal{V}^{\ell}_{r,0} \geq \vartheta^{\ell}_{r,1} + (\boldsymbol{\rho}^{g,\ell}_{r,1})^{\mathrm{T}} \boldsymbol{z}^{g}_{0}, \forall \ell \in [I-1] \tag{15a}$$

$$\mathcal{V}^{\ell}_{r,t} \geq \begin{cases} \vartheta^{\ell}_{r,t+1} + (\boldsymbol{\rho}^{g,\ell,copy}_{r,t+1})^{\mathrm{T}} \boldsymbol{z}^{g,copy}_{t} + (\boldsymbol{\rho}^{d,\ell}_{r,t+1})^{\mathrm{T}} \boldsymbol{z}^{d}_{t}, \text{if } t=1 \\ \vartheta^{\ell}_{r,t+1} + (\boldsymbol{\rho}^{g,\ell,copy}_{r,t+1})^{\mathrm{T}} \boldsymbol{z}^{g,copy}_{t} + (\boldsymbol{\rho}^{d,\ell}_{r,t+1})^{\mathrm{T}} \boldsymbol{z}^{d}_{t} \\ \qquad + (\boldsymbol{\rho}^{d,\ell,copy}_{r,t+1})^{\mathrm{T}} \boldsymbol{z}^{d,copy}_{t}, \text{if } t=2,...,T-2 \\ \vartheta^{\ell}_{r,t+1} + (\boldsymbol{\rho}^{g,\ell,copy}_{r,t+1})^{\mathrm{T}} \boldsymbol{z}^{g,copy}_{t}, \text{if } t=T-1 \\ \forall \ell \in [I-1] \end{cases} \tag{15b}$$

where I is the current iteration counter. $\vartheta^{\ell}_{r,t}$, $\boldsymbol{\rho}^{g,\ell,copy}_{r,t}$, $\boldsymbol{\rho}^{d,\ell}_{r,t}$ and $\boldsymbol{\rho}^{d,\ell,copy}_{r,t}$ are cut coefficients obtained by solving the Lagrangian dual problems of (16) in the backward step.

(2) Backward Step

In the backward step, by adding redundant variables $\boldsymbol{s}^{g,copy}_{t}$, $\boldsymbol{s}^{d}_{t}$, $\boldsymbol{s}^{d,copy}_{t}$ and redundant constraints into (14), we obtain

$$\begin{aligned} Q_t = \min g_t(\boldsymbol{x}_t, \boldsymbol{y}_t) + \gamma + \boldsymbol{\varphi}^{\mathrm{T}} \boldsymbol{\mu}\left(\boldsymbol{s}^{d,copy}_{t}, \boldsymbol{s}^{d}_{t}, \boldsymbol{x}_t\right) \\ + \left\langle \Sigma\left(\boldsymbol{s}^{d,copy}_{t}, \boldsymbol{s}^{d}_{t}, \boldsymbol{x}_t\right), \boldsymbol{\psi} \right\rangle_{\mathrm{F}} \\ \text{s.t.} \quad (11a)-(11c), (12), (13d), (15) \\ \boldsymbol{x}_t, \boldsymbol{y}_t \in \mathcal{X}_t\left(\boldsymbol{s}^{g,copy}_{t}, \boldsymbol{s}^{d,copy}_{t}, \boldsymbol{s}^{d}_{t}, \boldsymbol{\xi}_t\right) \\ \boldsymbol{z}^{g,copy}_{t} = M_t \boldsymbol{s}^{g,copy}_{t} \\ \boldsymbol{z}^{d,copy}_{t} = \begin{bmatrix} G_t \boldsymbol{s}^{d}_{t} \\ L_t \boldsymbol{s}^{d,copy}_{t} \end{bmatrix} \\ \boldsymbol{s}^{g,copy}_{t} = \boldsymbol{z}^{g,copy}_{t-1} : \boldsymbol{\rho}^{g,copy}_{I,r,t} \\ \boldsymbol{s}^{d}_{t} = \boldsymbol{z}^{d}_{t-1} : \boldsymbol{\rho}^{d}_{I,r,t} \\ \boldsymbol{s}^{d,copy}_{t} = \boldsymbol{z}^{d,copy}_{t-1} : \boldsymbol{\rho}^{d,copy}_{I,r,t} \\ 0 \leq \boldsymbol{s}^{g,copy}_{t}, \boldsymbol{s}^{d}_{t}, \boldsymbol{s}^{d,copy}_{t} \leq 1 \end{aligned} \tag{16}$$

By relaxing redundant constraints, the Lagrangian dual problem of (16) is formulated as

$$\begin{aligned} \mathcal{L}_t = \\ \max_{\boldsymbol{\rho}^{g,copy}_{I,r,t}, \boldsymbol{\rho}^{d}_{I,r,t}, \boldsymbol{\rho}^{d,copy}_{I,r,t}} \min g_t(\boldsymbol{x}_t, \boldsymbol{y}_t) + \gamma + \boldsymbol{\varphi}^{\mathrm{T}} \boldsymbol{\mu}\left(\boldsymbol{s}^{d,copy}_{t}, \boldsymbol{s}^{d}_{t}, \boldsymbol{x}_t\right) \\ + \left\langle \Sigma\left(\boldsymbol{s}^{d,copy}_{t}, \boldsymbol{s}^{d}_{t}, \boldsymbol{x}_t\right), \boldsymbol{\psi} \right\rangle_{\mathrm{F}} - \left(\boldsymbol{\rho}^{d,copy}_{I,r,t}\right)^{\mathrm{T}} \left(\boldsymbol{s}^{d,copy}_{t} - \boldsymbol{z}^{d,copy}_{t-1}\right) \\ - \left(\boldsymbol{\rho}^{d}_{I,r,t}\right)^{\mathrm{T}} \left(\boldsymbol{s}^{d}_{t} - \boldsymbol{z}^{d}_{t-1}\right) - \left(\boldsymbol{\rho}^{g,copy}_{I,r,t}\right)^{\mathrm{T}} \left(\boldsymbol{s}^{g,copy}_{t} - \boldsymbol{z}^{g,copy}_{t-1}\right) \\ \text{s.t.} \quad (11a)-(11c), (12), (13d), (15) \\ \boldsymbol{x}_t, \boldsymbol{y}_t \in \mathcal{X}_t\left(\boldsymbol{s}^{g,copy}_{t}, \boldsymbol{s}^{d,copy}_{t}, \boldsymbol{s}^{d}_{t}, \boldsymbol{\xi}_t\right) \\ \boldsymbol{z}^{g,copy}_{t} = M_t \boldsymbol{s}^{g,copy}_{t} \\ \boldsymbol{z}^{d,copy}_{t} = \begin{bmatrix} G_t \boldsymbol{s}^{d}_{t} \\ L_t \boldsymbol{s}^{d,copy}_{t} \end{bmatrix} \\ 0 \leq \boldsymbol{s}^{g,copy}_{t}, \boldsymbol{s}^{d}_{t}, \boldsymbol{s}^{d,copy}_{t} \leq 1 \end{aligned} \tag{17}$$

The outer problem of (17) is unbounded, which is generally solved by sub-gradient method. However, the sub-gradient method is time-consuming since it requires numerous iterations to obtain the optimal Lagrange multipliers. Thus, we replace Lagrangian cut by strengthened Benders cut [25]. The dual multipliers $\boldsymbol{\rho}^{g,copy}_{I,r,t}$, $\boldsymbol{\rho}^{d}_{I,r,t}$, $\boldsymbol{\rho}^{d,copy}_{I,r,t}$ in strengthened Benders cut are equal to the ones in Benders cut, which are calculated by solving the dual problem of (16) where all the binary variables are relaxed into continuous ones. Then cut coefficient $\vartheta_{I,r,t}$ is computed as (18) by solving the inner problem of (17) with obtained multipliers $\boldsymbol{\rho}^{g,copy}_{I,r,t}$, $\boldsymbol{\rho}^{d}_{I,r,t}$, $\boldsymbol{\rho}^{d,copy}_{I,r,t}$.

$$\begin{aligned} \vartheta_{I,r,t} = g_t(\boldsymbol{x}_t, \boldsymbol{y}_t) + \gamma + \boldsymbol{\varphi}^{\mathrm{T}} \boldsymbol{\mu}\left(\boldsymbol{s}^{d,copy}_{t}, \boldsymbol{s}^{d}_{t}, \boldsymbol{x}_t\right) \\ + \left\langle \Sigma\left(\boldsymbol{s}^{d,copy}_{t}, \boldsymbol{s}^{d}_{t}, \boldsymbol{x}_t\right), \boldsymbol{\psi} \right\rangle_{\mathrm{F}} - \left(\boldsymbol{\rho}^{d}_{I,r,t}\right)^{\mathrm{T}} \boldsymbol{s}^{d}_{t} \\ - \left(\boldsymbol{\rho}^{g,copy}_{I,r,t}\right)^{\mathrm{T}} \boldsymbol{s}^{g,copy}_{t} - \left(\boldsymbol{\rho}^{d,copy}_{I,r,t}\right)^{\mathrm{T}} \boldsymbol{s}^{d,copy}_{t} \end{aligned} \tag{18}$$

Based on the forward and backward steps with dummy variables, the cross-time stage variables and corresponding cutting planes can be passed stage by stage as Fig. 3 shows.

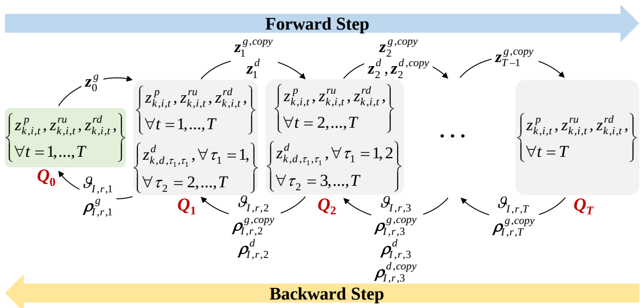

Fig. 3: Passed state variables and cutting planes via dummy variables.

The solution procedure of the improved SDDiP is shown in Algorithm 1. The algorithm converges theoretically until the lower bound LB reaches the statistical confidence interval of upper bound UB. The LB is the optimal objective value of the problem Q_0. The confidence interval representing UB is

$$\left[J - z_{\alpha/2}\frac{Z}{\sqrt{S}}, J + z_{\alpha/2}\frac{Z}{\sqrt{S}}\right] \tag{19}$$

where $z_{\alpha/2}$ is the $1-\alpha$ quantile of the standard normal distribution, S is the number of uncertainty paths, J and Z are the mean and the variance of UB, which are calculated by

$$J = f(\boldsymbol{x}_0, \boldsymbol{y}_0) + \frac{1}{S}\sum_{s=1}^{S}\sum_{t\in\mathcal{T}} g_t(\boldsymbol{x}_{s,t}, \boldsymbol{y}_{s,t}) \tag{20a}$$

$$Z = \sqrt{\frac{1}{S-1}\sum_{s=1}^{S}\left[f(\boldsymbol{x}_0, \boldsymbol{y}_0) + \sum_{t\in\mathcal{T}} g_t(\boldsymbol{x}_{s,t}, \boldsymbol{y}_{s,t}) - J\right]^2} \tag{20b}$$

To achieve a better optimality gap, the iteration stops when the gap between the supremum of the confidence interval and the LB is small enough. By implementing Algorithm 1 in day-ahead stage, the optimal power output and reserve capacity of thermal units and under-approximation cutting planes can be obtained. With these, the multistage scheduling of power systems can be implemented period-by-period. Specifically, when observing the uncertainty at current time period, the optimal intra-day dispatch decision can be calculated at once by solving the re-dispatch problems (14) with

Algorithm 1: Improved SDDiP with Dummy Variables

```
Initialize: Iteration account I ← 1, LB ← 0, UB ← +∞
while the stopping criterion is not satisfied do
    Sample S uncertainty paths ξ_{s,t} from the scenario tree
    *Forward step*
    for s = 1 : S do
        Solve the pre-dispatch problem Q_0; save the optimal
          solution {z_0^g, y_0}
        for t = 1 : T do
            Solve the re-dispatch problem Q_t; save the
              optimal solution {z_{s,t}^d, y_{s,t}, z_{s,t}^{g,copy}, z_{s,t}^{d,copy}}
        end
    end
    Update UB by (19)-(20)
    *Backward step*
    for t = T : 1 do
        for s = 1 : S do
            for r = 1 : N_t do
                Solve the Lagrangian dual problem (17);
                  collect cut coefficients and generate new
                  cutting planes by (15) for Q_{t-1}
            end
        end
    end
    Solve the pre-dispatch problem Q_0 and update LB
    I ← I + 1
end
```

$Q_{r,t+1}$ replaced by its under-approximation cutting planes. Thus, we only need to conduct Algorithm 1 one time in day-ahead (i.e., offline training) to obtain the optimal day-ahead decisions and cutting planes, which can be directly used for the real-time re-dispatch in intra-day without re-calculating them (i.e., online application).

4 Case Study

In this section, the proposed method is verified via numerical experiments on the IEEE 5-bus system and 118-bus system. All simulations are carried out by Julia language with JuMP package and Gurobi 10.1 on a computer with Intel(R) Xeon(R) Platinum 8338C CPU @ 2.60GHz and 256 GB RAM.

To show the advantage of the proposed multistage DRO method with decision-dependent ambiguity set, the following models are set for comparison.

Model 1: Multistage stochastic programming with fixed scenario probability distribution, solved by SDDP [8].

Model 2: Multistage robust optimization with decision-dependent uncertainty set, solved by linear affine policy and adaptive column-and-constraint generation algorithm [20].

Model 3: Traditional multistage distributionally robust optimization with decision-independent ambiguity set (i.e., set λ_d^{μ} and $\boldsymbol{\lambda}_d^{cov}$ to be 0), solved by improved SDDiP.

Model 4: Proposed multistage distributionally robust optimization with decision-dependent ambiguity set, solved by improved SDDiP.

4.1 IEEE 5-bus system

The IEEE 5-bus system contains 2 thermal generators, 1 wind farm, 1 deferrable load and 4 regular loads where 1 regular load is allowed to be curtailed. The parameters are given in Table 1. In the SDDiP algorithm, the size of discrete support N_t is chosen as 10 and the number of uncertainty path is 1. The dispatch period is 24 hours with 1 hour resolution.

Due to lack of real-world data, we generate sample data to calculate the coefficients λ_d^{μ} and $\boldsymbol{\lambda}_d^{cov}$. Specifically, the sample data of

Table 1 Parameters in IEEE 5-bus system.

Parameter	Value	Parameter	Value
P_i^u	[155, 80] MW	α_i	[17.26, 16.60] \$/MW
P_i^l	[70, 40] MW	$\beta_i^{\pm}$	[1.73, 1.66] \$/MW
R_i^u	[120, 60] MW	$d_i^{\pm}$	[1.73, 1.66] \$/MW
R_i^d	[120, 60] MW	c_m^s	3 \$/MWh
c^{ls}	500 \$/MWh	c_n^c	1 \$/MWh

wind power and baseline load comes from [26], and we modify the equation (1) as $D_{m,t}^s = \hat{D}_{m,t}^s + f_{m,t} \sum_{\tau=1}^{t-1} d_{m,\tau,t}^s, \forall m \in \mathcal{D}_s$ where $f_{m,t}$ is a random number used to characterize randomness, which follows a normal distribution with mean as 1 and standard deviation as 0.05. Note that there is no random coefficient before $\hat{D}_{m,t}^s$ since its randomness has been considered by different realizations in the sample data. Then the sample data of $f_{m,t}$ and $\sum_{\tau=1}^{t-1} d_{m,\tau,t}^s$ (follows uniform distribution) is generated by Monte Carlo Simulation. After that, we can calculate λ_d^{μ} and $\boldsymbol{\lambda}_d^{cov}$ via the data-driven approach given in Section 2.2.

(1) Convergence Performance

Fig. 4 shows the iteration process of the improved SDDiP algorithm. The algorithm converges after 24 iterations. With the iteration, the supremum and infimum of confidence interval gradually close. The gap between LB and the supremum of confidence interval reaches 0.82%. Thus, the improved SDDiP algorithm provides satisfactory convergence performance for the proposed multistage DRO model.

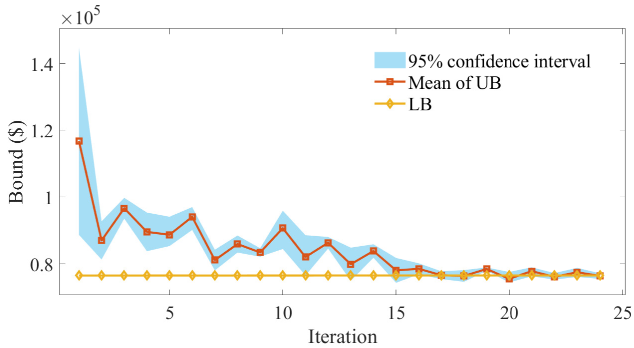

Fig. 4: Iteration process of improved SDDiP algorithm.

(2) Comparative Studies

(i) In-sample Performance Analysis

In-sample evaluation is conducted for model 1-4, which is the expected performance of total costs before uncertainty realizations. Table 2 presents the in-sample test results. Model 1 has the lowest in-sample expectation cost since it considers fixed probability distribution instead of the worst case. For model 2, the optimal decision distributes at the bound of uncertainty set. Thus, the solution is over-conservative and the expected total cost is highest among the four models. For model 3 and model 4, the total costs are between model 1 and mode 2. This is because the DRO method considers the worst-case probability distribution rather than the fixed one in SO or the worst-case scenario in RO, a trade-off between economics and robustness is obtained. Besides, model 4 has lower cost than model 3. This is because the demand shifting decisions can change the probability distribution parameters of random variables via the decision-dependent ambiguity set. Therefore, the probability of certain in-sample scenarios with lower cost increases, leading to lower expected cost.

Table 2 In-sample test results of model 1-4 on the IEEE 5-bus system.

	Model 1	Model 2	Model 3	Model 4
Times (s)	34.81	2.49	45.46	47.22
Generation cost ($)	76326.0	76333.2	76317.9	76320.6
Reserve cost ($)	354.5	1154.4	353.4	253.9
Expected re-dispatch cost ($)	784.8	13019.2	3037.0	2183.3
Total cost ($)	77465.3	90506.8	79708.3	78757.8

(ii) Out-of-sample Performance Analysis

For evaluating the real-world performance of model 1-4 under different uncertainty realizations, out-of-sample test is conducted in this subsection. Since our model is implemented in a multistage framework and the decisions at each stage will affect the uncertainty realizations of subsequent stages due to DDUs, the scenarios used for out-of-sample test are generated independently at each stage according to equations (3a)-(3b). Specifically, with obtained pre-dispatch strategies, the scenarios at stage 1 are generated by Monte Carlo simulation according to the mean and covariance matrix at stage 1. Under the generated scenarios, the demand shifting decisions at stage 1 are obtained by solving the problem Q_1. Then, the mean and covariance matrix at stage 2 can be calculated based on the decisions at stage 1 and equations (3a)-(3b), which are used to generate the test scenarios for stage 2. The out-of-sample test will be done by implementing the above steps until stage T. Because the under-approximation cutting planes of $Q_{r,t+1}$ are obtained by day-ahead offline training, the re-dispatch problem Q_t can be calculated directly and quickly in real-time re-dispatch.

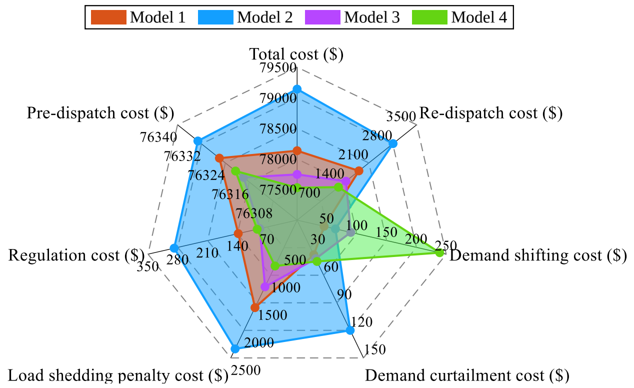

Fig. 5: The result of out-of-sample test for model 1-4.

Fig. 5 shows the economic performance of model 1-4 in the out-of-sample test. As expected, model 3 and model 4 have lower total cost than model 1 and 2 due to the advantages of DRO over SP and RO. For model 2, the solution is derived under the worst-case scenarios, which is conservative. More importantly, affine policy over simplifies the model. The re-dispatch decisions are directly determined by the linear product of affine coefficients and uncertainty realizations. The feasible region of decision variables is greatly limited by the linear mapping structure and is not equal equivalent to that of original multistage model. Thus, the solution quality of model 2 reduces, resulting in highest cost among the four models. Model 1 and model 3 has similar cost distribution because they are both formulated based on decision-independent probability distribution, where one is under the fixed PDF while one is under the worst-case PDF. For model 4, the demand shifting cost is obviously higher than the other models. This is because the probability distribution of future scenarios is coupled with demand shifting decisions. Therefore, more demand shift are implemented to increase the occurrence probability of scenarios with lower cost, thus reducing total cost.

(iii) Sensitivity Analysis

In the following, the impacts of three factors are investigated: the decision-dependency coefficients λ_d^{μ} and $\boldsymbol{\lambda}_d^{cov}$, the size of discrete support N_t, the number of uncertainty paths in SDDiP algorithm.

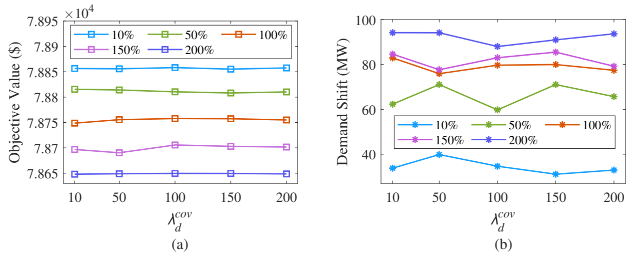

Fig. 6: Expected dispatch cost and demand shifting of model 4 under different decision-dependency coefficients λ_d^{μ} and $\boldsymbol{\lambda}_d^{cov}$.

First, the decision-dependency coefficients λ_d^{μ} and $\boldsymbol{\lambda}_d^{cov}$ are set as 10%, 50%, 100%, 150%, and 200% of their default values in Section 4.1. The simulation results of model 4 are shown in Fig. 6. The single line in the figure represents the result under a certain value of λ_d^{μ}, and the point in a single line is the result under different $\boldsymbol{\lambda}_d^{cov}$. It can be found that the expected cost decreases and the demand shift increases with the parameter λ_d^{μ} increases. Since the total cost can be reduced by implementing demand shift as Fig. 4 shows and the higher λ_d^{μ} represents greater impacts of demand shifting decision on the uncertainty parameters of deferrable loads in (3a)-(3b), more demands are shifted when λ_d^{μ} is large to decrease total cost. Besides, $\boldsymbol{\lambda}_d^{cov}$ has not a linear impact on the expected cost and demand shift as the curves fluctuate with $\boldsymbol{\lambda}_d^{cov}$ increases.

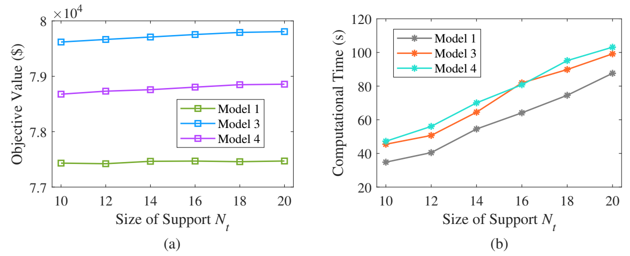

Fig. 7: Expected cost and computational time under different size of support.

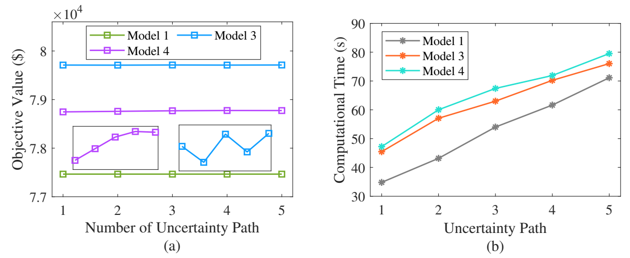

Fig. 8: Expected cost and computational time under different number of uncertain paths.

Then we investigate the impact of the size of discrete support N_t and the number of uncertainty paths. Here, model 2 is excluded since it is not affected by the two factors. As Fig. 7 shows, the total costs of model 3 and 4 increases when the size of support becomes larger. Because the probability distribution is strictly limited by the three constraints in (3a)-(3b), larger support allows greater fluctuations in the probability of a single scenario. Thus, the scenario probability tends to a worse distribution, resulting in higher cost. The computational time increases with larger support due to more calculation in the backward step. In Fig. 8, the expected cost remains almost stable with negligible fluctuation. However, the computational time increases significantly with larger number of uncertainty path, which is because more calculations are needed in the forward and backward steps of the SDDiP algorithm.

4.2 IEEE 118-bus system

To show the scalability of the proposed method, the IEEE 118-bus system is used for the test. The whole system has 54 thermal generators, 10 wind farms, 186 transmission lines, 5 deferrable loads and 5 curtailable loads. The data of the system is at http://motor.ece.iit.edu/data/JEAS_IEEE118.doc.

Table 3 In-sample and out-of-sample tests on the IEEE 118-bus system.

	Model 1	Model 2	Model 3	Model 4
Times (min)	12.58	3.78	14.37	13.75
In-sample cost ($)	1,438,860	1,639,593	1,502,017	1,477,425
Out-of-sample cost ($)	1,485,562	1,503,754	1,473,902	1,462,214

Table 3 shows the simulation results. With the increase of problem scale, the computation time of all models increases. However, since the SDDiP algorithm is conducted in day-ahead and the well trained cutting planes can be directly used in intra-day real-time scheduling, the computational time is acceptable. In term of economic performance, as what is expected, model 4 still performs best with the lowest out-of-sample cost among the four models. Thus, the proposed method has good scalability for large-scale power systems.

5 Conclusion

This paper proposes a multistage DRO method for generation dispatch with DR, where the DDUs of deferrable loads and the DIUs of wind power and regular loads are considered. A novel decision-dependency ambiguity set with a data-driven approach is developed to formulate both DDUs and DIUs and obtain decision-dependency coefficients, with which a multistage DRO model is established for the generation dispatch problem. The strong duality theory, binary expansion and McCormick envelope are adopted to transform the model into a tractable MILP. Then an improved SDDiP algorithm is designed to effectively solve the model. Case studies compare the proposed multistage DRO model with multistage SP, RO and decision-independent DRO methods. The results show that the proposed method can obtain lower dispatch cost than the other three methods. Besides, the tests on the IEEE 118-bus system illustrates that the proposed approach has good scalability for large-scale power systems.

6 References

1 Zheng, S., Sun, Y., Li, B., Hu, Y., Qi, B., Shi, K., et al.: 'Stochastic programming model for incentive-based demand response considering complex uncertainties of consumers', *IET Generation, Transmission & Distribution*, 2020, **14**, (20), pp. 4488–4500

2 Wang, Y., Liang, H., Dinavahi, V.: 'Two-stage stochastic demand response in smart grid considering random appliance usage patterns', *IET Generation, Transmission & Distribution*, 2018, **12**, (18), pp. 4163–4171

3 Du, G., Zhao, D., Liu, X., Wu, Z., Li, C.: 'Decentralized robust dispatch for multi-area ac/dc system considering wind power uncertainty', *IET Generation, Transmission & Distribution*, 2021, **15**, (19), pp. 2710–2721

4 Liu, G., Starke, M., Xiao, B., Tomsovic, K.: 'Robust optimisation-based microgrid scheduling with islanding constraints', *IET Generation, Transmission & Distribution*, 2017, **11**, (7), pp. 1820–1828

5 Chen, Y., Wang, J., Wang, S., Bo, R., Gu, C., Li, Q.: 'Managing reserve deliverability risk of integrated electricity-heat systems in day-ahead market: A distributionally robust joint chance constrained approach', *IET Generation, Transmission & Distribution*, , **n/a**, (n/a)

6 Shi, Z., Liang, H., Dinavahi, V.: 'Distributionally robust multi-period energy management for cchp-based microgrids', *IET Generation, Transmission & Distribution*, 2020, **14**, (19), pp. 4097–4107

7 Qiu, H., Gu, W., Ning, C., Lu, X., Liu, P., Wu, Z.: 'Multistage mixed-integer robust optimization for power grid scheduling: An efficient reformulation algorithm', *IEEE Transactions on Sustainable Energy*, 2023, **14**, (1), pp. 254–271

8 Lu, R., Ding, T., Qin, B., Ma, J., Fang, X., Dong, Z.: 'Multi-stage stochastic programming to joint economic dispatch for energy and reserve with uncertain renewable energy', *IEEE Transactions on Sustainable Energy*, 2020, **11**, (3), pp. 1140–1151

9 Ding, T., Qu, M., Huang, C., Wang, Z., Du, P., Shahidehpour, M.: 'Multi-period active distribution network planning using multi-stage stochastic programming and nested decomposition by sddip', *IEEE Transactions on Power Systems*, 2021, **36**, (3), pp. 2281–2292

10 G. Cobos, N., Arroyo, J.M., Alguacil, N., Street, A.: 'Network-constrained unit commitment under significant wind penetration: A multistage robust approach with non-fixed recourse', *Applied Energy*, 2018, **232**, pp. 489–503

11 Qiu, H., Wang, L., Gu, W., Pan, G., Ning, C., Wu, Z., et al.: 'Multistage scheduling of regional power grids against sequential outage and power uncertainties', *IEEE Transactions on Smart Grid*, 2022, **13**, (6), pp. 4624–4637

12 Qiu, H., Gu, W., Sheng, W., Wang, L., Sun, Q., Wu, Z.: 'Resilience-oriented multistage scheduling for power grids considering nonanticipativity under tropical cyclones', *IEEE Transactions on Power Systems*, 2022, pp. 1–14

13 Ding, T., Zhang, X., Lu, R., Qu, M., Shahidehpour, M., He, Y., et al.: 'Multi-stage distributionally robust stochastic dual dynamic programming to multi-period economic dispatch with virtual energy storage', *IEEE Transactions on Sustainable Energy*, 2022, **13**, (1), pp. 146–158

14 Giannelos, S., Konstantelos, I., Strbac, G.: 'Option value of demand-side response schemes under decision-dependent uncertainty', *IEEE Transactions on Power Systems*, 2018, **33**, (5), pp. 5103–5113

15 Yin, W., Feng, S., Hou, Y.: 'Stochastic wind farm expansion planning with decision-dependent uncertainty under spatial smoothing effect', *IEEE Transactions on Power Systems*, 2023, **38**, (3), pp. 2845–2857

16 Zhang, W., Shao, C., Hu, B., Xie, K., Siano, P., Li, M., et al.: 'Transmission defense hardening against typhoon disasters under decision-dependent uncertainty', *IEEE Transactions on Power Systems*, 2023, **38**, (3), pp. 2653–2665

17 Hu, B., Pan, C., Shao, C., Xie, K., Niu, T., Li, C., et al.: 'Decision-dependent uncertainty modeling in power system operational reliability evaluations', *IEEE Transactions on Power Systems*, 2021, **36**, (6), pp. 5708–5721

18 Zhang, Y., Liu, F., Wang, Z., Su, Y., Wang, W., Feng, S.: 'Robust scheduling of virtual power plant under exogenous and endogenous uncertainties', *IEEE Transactions on Power Systems*, 2022, **37**, (2), pp. 1311–1325

19 Chen, Y., Wei, W.: 'Robust generation dispatch with strategic renewable power curtailment and decision-dependent uncertainty', *IEEE Transactions on Power Systems*, 2022, pp. 1–14

20 Su, Y., Liu, F., Wang, Z., Zhang, Y., Li, B., Chen, Y.: 'Multi-stage robust dispatch considering demand response under decision-dependent uncertainty', *IEEE Transactions on Smart Grid*, 2022, pp. 1–1

21 Xian, Y., Shen, S.: 'Multistage distributionally robust mixed-integer programming with decision-dependent moment-based ambiguity sets', *Mathematical Programming*, 2022, **196**, pp. 1025–1064

22 Li, K., Wang, Y., Zhang, N., Wang, F.: 'Precision and accuracy co-optimization-based demand response baseline load estimation using bidirectional data', *IEEE Transactions on Smart Grid*, 2023, **14**, (1), pp. 266–276

23 Chen, Y., Chen, C., Zhang, X., Cui, M., Li, F., Wang, X., et al.: 'Privacy-preserving baseline load reconstruction for residential demand response considering distributed energy resources', *IEEE Transactions on Industrial Informatics*, 2022, **18**, (5), pp. 3541–3550

24 Birant, D., Kut, A.: 'St-dbscan: An algorithm for clustering spatial-temporal data', *Data Knowledge Engineering*, 2007, **60**, (1), pp. 208–221. intelligent Data Mining

25 Zou, J., Ahmed, S., Sun, X.A.: 'Stochastic dual dynamic integer programming', *Mathematical Programming*, 2019, **175**, pp. 461–502

26 Guo, Z., Wei, W., Shahidehpour, M., Chen, L., Mei, S.: 'Two-timescale dynamic energy and reserve dispatch with wind power and energy storage', *IEEE Transactions on Sustainable Energy*, 2023, **14**, (1), pp. 490–503